Paper
Int'l J. of Aeronautical & Space Sci. 16(4), 520–528 (2015)
DOI: http://dx.doi.org/10.5139/IJASS.2015.16.4.520

IJASS
International Journal of Aeronautical and Space Sciences

Experimental Study on the Performance of a Bidirectional Hybrid Piezoelectric-Hydraulic Actuator

Xiao Long Jin, Ngoc San Ha, Yong Zhe Li and Nam Seo Goo*

Department of Advanced Technology Fusion, Konkuk University, Seoul 05029, Republic of Korea

Jangmi Woo, Han Seo Ko**

Department of Mechanical Engineering, Sungkyunkwan University, Gyeonggi-do 16419, Republic of Korea

Tae Heun Kim***

Firtec. Co., Gyeongsangnam-do 51528, Republic of Korea

Chang Seop Lee****

Agency for Defense Development, Daejeon 34060, Republic of Korea

Abstract

The piezoelectric-hydraulic actuator is a hybrid device that consists of a hydraulic pump driven by a piezo-stack coupled to a conventional hydraulic cylinder. The actuator is of compact size, but can produce a moderate energy output. Such hybrid actuators are currently being researched and developed in many industrialized countries due to the requirement for high performance and compact flight systems. In a previous study, we designed and manufactured a unidirectional hybrid actuator. However, the blocking force was not as high as expected. Therefore, in this study, we redesigned the pump chamber and hydraulic cylinder and also improved the system by removing the air bubbles. Two different types of piezo-stacks were used. In order to achieve bidirectional capabilities in the actuator, commercial solenoid valves were used to control the direction of the output cylinder. Experimental testing of the actuator in unidirectional and bidirectional modes was performed to examine performance issues related to driving frequency, bias pressure, reed valve thickness, etc. The results showed that the maximum blocking force was measured as 970.2N when the frequency was 185Hz.

Key words: Hybrid actuator, Piezo-stack driven pump, Blocking force, Bidirectional valve system

1. Introduction

A piezoelectric-based hydraulic actuator is a hybrid device for a hydraulic pump driven by piezoelectric stacks. It is also coupled to a conventional hydraulic cylinder via a set of fast-acting valves. Smart materials based hybrid actuators are actively being researched and developed in many developed countries due to the requirement for high performance and compact flight systems. These smart material driven electro-hydraulic actuators have been constructed to investigate their behavior and verify the blocking force and output velocity. Because various sized driving elements have been used, the performance results differ in each case.

So far, according to the development of the smart material driven electro-hydraulic actuator, the first reported hybrid hydraulic actuator was developed by Konishi et al. [1]. This actuator driven by a piezo-stack had a power output of 34W and a peak driving frequency of 300Hz. In recent times, many

* Professor, Corresponding author: nsgoo@konkuk.ac.kr
** Professor
*** Research engineer
**** Researcher

Received: July 2, 2015 Accepted: Demcember 3, 2015

http://ijass.org pISSN: 2093-274x eISSN: 2093-2480

researchers have developed actuators using smart materials [2-6]. Mauck and Lynch developed an actuator driven by PZT (lead zirconium titanate) piezo-stack material [5], with the actuator consisting of a reciprocating piezoelectric pump and passive check valves. The maximum velocity and blocking force of 72.5mm/s and 271N, respectively, was achieved under 800 Volt, 2.41 MPa accumulator pressure, and 60Hz driving frequency. Chaudhuri and Wereley developed their compact hybrid actuation system using the single-crystal electrostrictive material PMN-32%PT [6]. The no-load testing of this actuator showed that the maximum output velocity was 330mm/s at 700Hz driving frequency. In a recent study, Zhefeng Xuan et al. developed an integrated hybrid hydraulic actuator driven by piezo-stacks [7]. Two types of piezo-stacks, P-025.40P of PI, Inc. and PSt 1000/25/80 of Piezomechanik, were tested. The maximum blocking force was 346N and the no-load velocity was 101mm/s at 250Hz when a Pst 1000/25/80 type piezo-stack was used as the driving material.

Until now, the maximum output velocity of an actuator driven by PMN-PT was 330mm/s, and a maximum blocking force of around 346N was obtained for the piezoelectric-based actuator. This means that PMN-PT can produce greater displacement, and the piezoelectric ceramics (PZT) can produce large stress. The elastic modulus of PMN-PT is much lower than PZT, and some researchers have reported that PMN-PT is not good at driving high blocking force actuators. Also, performance degradation occurs when the temperature increases. Therefore, the correct selection of a smart structure for an actuator depends on the purpose of attaining a maximum blocking force or maximum output velocity. In our previous study, the PZT was used as a driving material for a unidirectional hybrid actuator to obtain a high blocking force [7]. However, the blocking force was not as high as expected. Therefore, the system needed to be redesigned and improved.

In this research, the aim was to develop a bidirectional piezoelectric-hydraulic actuator with a large blocking force based on the design of a unidirectional hybrid actuator [7]. In order to improve the blocking force, the dimensions of the pump chamber and cylinder were redesigned. In addition, two types of piezo-stack (PZT), P-025.40P of PI, Inc. and Pst 1000/25/80 of Piezomechanik, were also used as the driving material, and a solenoid valve was used to achieve a bidirectional motion for the actuator. However, the bidirectional system was more complicated than the unidirectional one. It appeared that air bubbles were developed inside the oil. The effort to remove air bubbles was initiated, and then the performance of the bidirectional actuator was re-evaluated.

2. The design of the bidirectional piezoelectric hybrid actuator

2.1 Configuration of the whole system

In this research, a bidirectional piezoelectric hybrid actuator was designed. Figure 1 shows the configuration of the actuator. The bidirectional hybrid actuator system has three main components: the piezoelectric pump, the solenoid valve, and the cylinder.

The piezoelectric pump can provide output pressure to drive the piston inside the cylinder through the smart material. Meanwhile, the function of the solenoid valve is to change the direction of the fluid so that the direction of the cylinder can be controlled. The pump assembly consists of a pump chamber, a reed valve, and the piezo-stack, as shown in Fig. 2. Two different types of piezo-stacks were used in this study, and their properties are listed in Table 1. The reed valve made of spring steel and sandwiched between two stainless steel plates was used in the pump part. This configuration allows only a unidirectional valve opening. When the fluid flows into the chamber from the inlet valve, the outlet valve port does not allow any fluid to come into the chamber and vice versa [9]. In this research, 0.05mm, 0.08mm, and 0.15mm thicknesses of reed valve were considered for the performance experiment.

The solenoid valve was used to achieve the bidirectional motion of the actuator. The solenoid valve was controlled by the NI LabVIEW program and relays. The two signal lights on the solenoid valve show the different directions of the cylinder when they are switched on, and both lights cannot

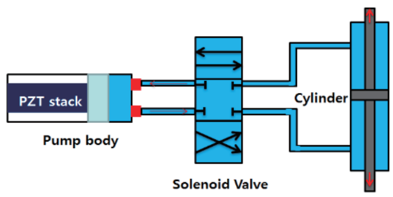

Fig. 1. Configuration of bidirectional hybrid actuator system

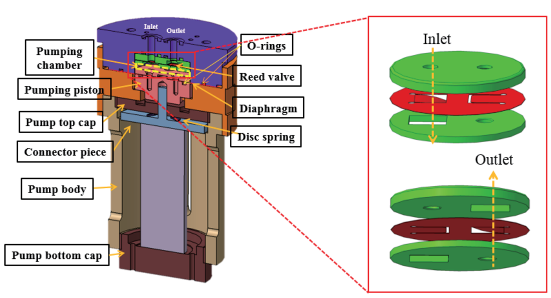

Fig. 2. Section view of the pump assembly

be on at the same time.

The working principle of piezoelectric hydraulic actuator is similar to that of micro-pump, but the difference between them is that the piezoelectric hydraulic actuator is closed system while the micro-pump is open system [10]. The operation of the system can be divided into four stages. The first stage is the compression stage. With both valves closed, the piezo-stack pushes hydraulic fluid into the closed pump chamber, resulting in pressure increasing in the chamber. The second stage is the exhaustion stage. The outlet valve opens, and the hydraulic fluid starts to flow out from the chamber into the output cylinder, resulting in motion in the output shaft. The third stage is the expansion stage. The piezo-stack starts to retreat, causing a pressure drop in the pumping chamber. The last stage is the intake. The inlet valve opens, and the low pressure driven side of the output cylinder moves back into the chamber. These four stages are repeated every pumping cycle, which result in a net mass flow rate out of the pump through the outlet tube and an equivalent mass flow rate into the pump through the inlet tube.

2.2 Design of actuator

In a previous study, the size of the piezo-stack (60×25mm^2) and pump chamber diameter (32mm) were designed based on the cylinder diameter, specified no-load velocity, and blocking force. Therefore, in this study, we used the size of the piezo-stack (60×25mm^2) to redesign the size of the pumping chamber and cylinder to get the maximum blocking force. The relationship between the blocking force, pumping chamber, and cylinder diameter was obtained using the formula in Chaudhuri and Wereley [11]. The bulk modulus of the fluid has a significant influence on the pressure from the piezoelectric pump and should be considered, when modeling the inside of the actuator,. The bulk modulus of the fluid can be calculated as equation (1). The bulk modulus decreases sharply due to the air in the fluid [12] as follows:

$$\beta_{eff} = -\frac{V\Delta P}{\Delta V} = -\frac{V\Delta P}{(\Delta V_{fluid} + \Delta V_{air} + \Delta V_{tube})} = \frac{1}{(\frac{1-\chi}{\beta_{fluid}} + \frac{\chi}{\beta_{air}} + \frac{D}{tE})} \quad (1)$$

where β_{eff}, β_{fluid}, and β_{air} are the effective, fluid, and air bulk modulus, respectively, χ is the air content percentage, t is the tube thickness, D is the tube diameter, and E is the modulus of elasticity.

The high bulk modulus of the fluid enhances the fluid stiffness and resonant frequency of the fluid flow and reduces pressure loss. The reduction of the bulk modulus is mainly due to the air in the fluid, the O-ring, and the flexibility of the tube. To increase the bulk modulus, the air in the system needs to be removed, the system needs to be cleaned, and a high bias pressure needs to be added. However, a high bias pressure disturbs the performance of the actuator, so it should be added moderately. In this study, the bulk modulus was chosen as 0.2GPa with the assumption of 2MPa bias pressure and 1% air contents[7].

The stiffness of the pump chamber is calculated using equation (2), where P_{pump}, $A_{chamber}$, and $L_{chamber}$ refer to the output pressure, the area of the pump chamber, and the length of the pump chamber, respectively.

$$K_{chamber} = \frac{\beta A_{chamber}}{L_{chamber}} \quad (2)$$

The displacement and blocking force from the piezo-stack can be calculated using equations (3) and (4), respectively. Here, K_{stack} and $K_{chamber}$ are the stiffness of the piezo-stack and the pump chamber, respectively, δ_0 is the displacement from the piezo-stack in the loaded condition, δ_{ftee} refers to the free condition, F_0 is the blocking force from the piezo-stack, and F_b is the maximum blocking force of the piezo-stack. The pressure output from the pump can be calculated using equation (5). Elements such as the losses in the fluidic system due to viscosity, compressibility, inertia, dynamics of lead valve, and friction in the output cylinder are not considered here [13].

$$\delta_0 = \frac{K_{stack}}{K_{stack} + K_{chamber}} \delta_{free} \quad (3)$$

$$F_0 = F_b - \delta_0 K_{stack} \quad (4)$$

$$P_{pump} = \frac{F_0}{A_{chamber}} \quad (5)$$

Table 1. Piezo-stack properties used in the hybrid actuator

Type	Size (mm)	Maximum displacement (μm)	Blocking force (N)	Capacitance (nF)	Maximum driving voltage (V)	Resonant frequency (kHz)
P-025.40P	60×25(Lx∅)	70/60	13000	1300	1000	19
Pst 1000/25/80	72×25(Lx∅)	105/80	20000	1700	1000	15

*Data was taken from [8]

The movement of the cylinder determines the total performance of the actuator. Therefore, the diameter of the cylinder has a significant effect on the blocking force and velocity. The blocking force is considerably enhanced by increasing the diameter of the cylinder, as shown in equations (6) and (7) below, while it is not affected by the diameter of the pump chamber. Here, $A_{ext} = \pi((d_{cylinder})^2 - (d_{shaft})^2)/4$, $d_{cylinder}$, and d_{shaft} are the diameter of the cylinder and shaft, respectively. The output fluid flow is calculated using equation (7), where Q_{pump} is the volume flow of the pump, and V_{ext} is the output velocity.

$$F_{ext} = P_{pump} A_{ext} \tag{6}$$

$$V_{ext} = \frac{Q_{pump}}{A_{Aext}} \tag{7}$$

From equations (2) to (7), we can get the relationship between blocking force, pumping chamber, and diameter of the cylinder. Figure 3 shows that increasing the diameter of the cylinder and decreasing the diameter of the pump chamber can obtain a higher performance. In this study, the target blocking force was 1500N. Finally, we selected the optimum diameters of the pump chamber and the cylinder as 30mm and 21mm, respectively.

2.3 Numerical Analysis

For the numerical analysis of a hybrid piezoelectric-hydraulic actuator, ANSYS CFX 13.0 software was used. Because a hybrid piezoelectric-hydraulic actuator transmits power from the movement of a piezo-hydraulic pump to a hydraulic cylinder through the fluid using a flow control valve, fluid-structure interaction (FSI) was used to consider the movements of the valve as well. FSI was heavily used to solve many complex engineering problems such as helicopter [14], high-speed printing machine [15]. FSI can be divided into 1-way, which makes structural analysis based on the results of flow analysis, and 2-way, which makes numerical analysis based on the interaction between the flow and structural analysis results [16]. Two kinds of governing equations were used for numerical analysis: one was for flow analysis and another was for structural analysis. The equations used for flow analysis were continuity equation (8), momentum equation (9), and energy equation (10):

$$\frac{\partial \rho}{\partial t} + \nabla \cdot (\rho \boldsymbol{U}) = 0 \tag{8}$$

$$\frac{D(\rho \boldsymbol{U})}{Dt} = -\nabla p + \nabla \cdot \boldsymbol{\tau} + \rho \boldsymbol{g} + \boldsymbol{S_M} \tag{9}$$

$$\frac{\partial(\rho h_{tot})}{\partial t} + \nabla \cdot (\rho \boldsymbol{U} h_{tot}) = \nabla \cdot (k \nabla T) + \nabla \cdot (\boldsymbol{\tau} \cdot \boldsymbol{U}) + \boldsymbol{U} \cdot \boldsymbol{S_M} + S_E \tag{10}$$

where ρ is the density of working fluid, t is the time, U is the flow rate vector, τ is shear stress vector of fluid, S_M is the momentum, h_{tot} is the enthalpy and S_E is the energy source. $\nabla \cdot (\boldsymbol{\tau} \cdot \boldsymbol{U})$ is the work generated by the viscous force, and $U \cdot S_M$ represents the work caused by an external movement source.

The governing equations for the structural analysis are the equilibrium equation (11), constitution equation (12), and compatibility equations (13) and (14) at the fluid and solid interface:

$$\rho_s \ddot{\boldsymbol{d}}_s = \nabla \cdot \boldsymbol{\sigma_s} + \boldsymbol{f_s} \tag{11}$$

$$\boldsymbol{\sigma_s} = \boldsymbol{D} \boldsymbol{\varepsilon_s} \tag{12}$$

$$\boldsymbol{\tau} \cdot \mathbf{n} = \boldsymbol{\tau_s} \cdot \mathbf{n_s} \tag{13}$$

$$\boldsymbol{\delta} = \boldsymbol{0} \tag{14}$$

where ρ_s is the density of solid, d_s is the displacement vector of solid, f_s is body force vector of solid, σ_s is stress vector, ε_s is the strain vector, D is the material constant matrix, and τ_s is the shear stress vector of solid, and δ is the displacement compatibility vector.

2.4 Experiment setup

Figure 4 shows the experiment setup. The pump assembly, the solenoid valve, and the cylinder are to the left. The middle shows the vacuum system and the oil pump, while to the

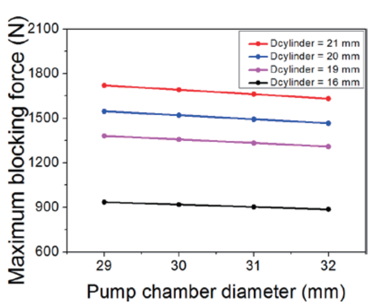

Fig. 3. Relationship between maximum blocking force and pump chamber diameter with different cylinder diameters

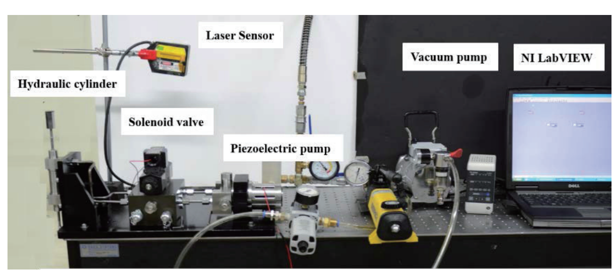

Fig. 4. Actual photo of bidirectional piezoelectric hybrid actuator set up

right, the LabVIEW program running on a laptop is in view. The laser sensor was also included for the displacement measurement of the hydraulic cylinder.

The actuating performance was measured after the piezoelectric-hydraulic actuator was assembled. First, the displacement of the output cylinder shaft was measured using a laser sensor in a no-load condition, and the measured displacement was divided by driving time to get the velocity of the output device. In the loading case, the external load was hung on the underside of the output cylinder shaft to measure the blocking force. The measurement method of velocity in the loading case was the same as in the no-load condition.

3. Results and discussion

3.1 Test with PI P-025.40P piezo-stack

Figures 5 and 6 show preliminary results that the maximum velocity of the cylinder rod is around 50.9mm/s when the frequency is 250Hz. No-load up and down velocities mean the cylinder velocity runs in a bidirectional motion. Figure 5 shows that the performances of the actuator

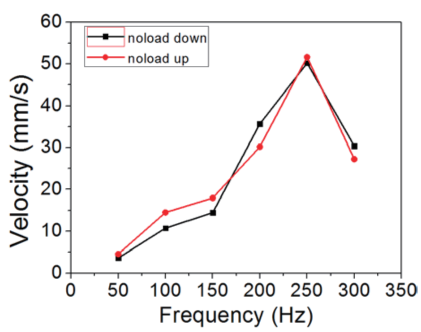

Fig. 5. Output up and down velocities with different driving frequencies in a no-load test at 2MPa bias pressure and 0.05mm thickness of reed valve

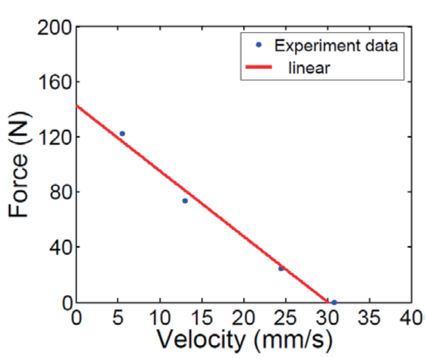

Fig. 6. Output force vs. velocity diagram with 1000V applied voltage and 200Hz driving frequency in an external loaded test

in two directions are fairly similar and that the bidirectional motion is achieved. Consequently, only the performance in one direction for the other measurements was measured. Figure 6 shows the maximum blocking force of 142N when the frequency was 200Hz and voltage was 1000V.

The preliminary result of the blocking force was not as good as the expected performance. The reason for the poor performance was found to be the result of a vacuum problem. The system of the bidirectional piezoelectric hybrid actuator is more complicated than the unidirectional actuator system [7]. When the bias pressure was included, air bubbles were developed in the oil. It was difficult to remove the air from one port on the piezo-hydraulic pump's side. In order to solve the problem regarding the air bubble in the actuator, a new cylinder was designed based on the old one, as shown in Fig. 7. The new cylinder was the same size as the original cylinder. However, two new ports were added at the two sides of the cylinder so that the air could be removed from these positions. The red circles in Figure 7 show the new ports. The new cylinder configuration improves the actuator performance significantly because the configuration can considerably reduce the amount of air bubbles, and it can maintain a stable internal environment.

After improving the cylinder, the performance of the actuator was measured. However, in order to obtain a more accurate blocking force, a load-cell (ENSTECH SCM-100K) was used. Before testing the actuator, the accuracy of the measuring system with the load cell was calibrated. The results showed that the error of this measuring system is 0.015kg. Therefore, this measuring system is suitable for testing the actuator.

The running time is the time at which the cylinder rod pushes the load-cell after the piezoelectric hydraulic actuator turns on. In this research, five running times were tested: 3s, 5s, 7s, 10s, and 12s at the frequency of 50Hz and voltage of 1000V. Figure 8 shows that the blocking force increased when the running time was increased. However, after 10s, the blocking force decreased because of the limited oil supply. The system needs time to become stable when it

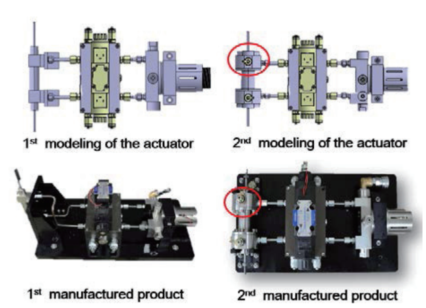

Fig. 7. System before and after improving the cylinder

is working. Therefore, a running time of 10s was selected for the other experiment.

Figure 9 shows the maximum blocking force with the different frequencies and running time (10s). The system worked stably after the new cylinder was used because almost all the air inside of the chamber, cylinder, and the whole system could be removed. The maximum blocking force was measured as 801.3N when the frequency was 185Hz.

In this study, 50~300Hz frequency was selected for the experiment. The natural frequency of the spring steel reed valves, 8.01mm long × 7.01mm wide × 0.1mm thick vibrating in air, was 1300Hz. The presence of a dense hydraulic fluid reduced the resonant frequency drastically. Using empirical relations [17] for the dynamic properties of reed valves, we were able to recalculate the vibrating frequency of a reed valve in fluid to be 530Hz. If the driving frequency is higher than the resonant frequency in fluid, the performance of a reed valve decreases, leading to a decrease in pump performance.

The power amplifier was automatically turned off when the frequency was higher than 300Hz because of the circuit protection inside. To validate the current limit, the amplifier and piezo-stack were modeled as a capacitor driven by an electrical source. The theoretical prediction of maximum frequency was predicted by equation (15). The maximum frequency was calculated as 245Hz, which was different from the actual results of 300Hz. The slight difference between theory and experiment results is because the voltage in sinusoidal form was assumed in theoretical calculation, while the voltage in rectangular form was used in the experiment [18].

$$f_{max} = \frac{I_{max}}{2\pi \cdot C \cdot V_{max}} \tag{15}$$

Tests were also carried out under load to investigate the performance of the actuator. The experimental setup is shown in Fig. 10. An external load was attached to one side of the cylinder while the displacement laser sensor was focused on the other side of the cylinder to measure the velocity. A dead load from 7.5kg to 32.5kg was fixed to the output piston shaft using pulley string and couplers. A weight smaller than 32.5kg was used in this research because of the length limit of the load shaft.

The load tests were performed at two kinds of bias pressure (1MPa, 2MPa) and three different frequencies (150Hz, 185Hz, 200Hz). The applied voltage of 1000V and 0.05mm thickness of reed valve were used in this experiment. Output velocities were measured with loads acting on the actuator, which can lead to a force-velocity curve. As the final result, the maximum blocking forces of each condition were also included as points on the force axis in Fig. 11 and Fig. 12. The 1MPa bias pressure tended to obtain high velocity, while 2MPa tended to obtain a large blocking force. Although increasing the bias pressure would decrease the fluid compliance or increase the fluid bulk modulus, it does not ensure a better performance. This is because a mismatch between the mechanical impedances of the driving material and pressurized fluid chamber can lead to a decrease in the actual induced strain in the driving material at an excessive bias pressure. In addition, the force was inversely proportional to velocity, and the curve had two folds, in which the bifurcation point was 7.5kg. These curves also went through the maximum force that was measured by

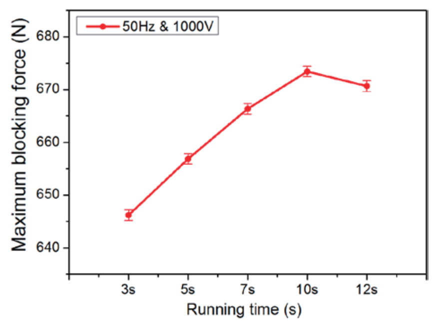

Fig. 8. Performance of maximum blocking force with 50Hz at 2MPa bias pressure and 0.05mm thickness of reed valve

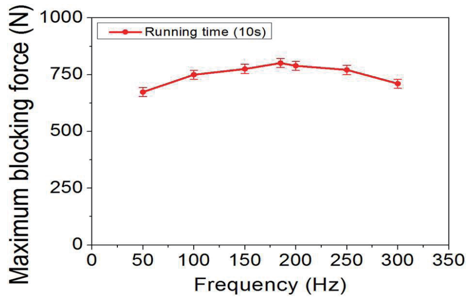

Fig. 9. Maximum blocking force with 10s running time at 2MPa bias pressure and 0.05mm thickness of reed valve

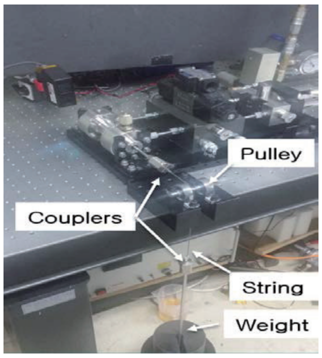

Fig. 10. Loading system to measure force-velocity relation

the load cell. However, for the higher external load masses (over 12.5kg), where the output displacement (and velocity) become very small, the force-velocity curve becomes an asymptote to the load axis. This is probably because of (i) the increasing effects of stiction and (ii) changes in the fluid bulk modulus because of a higher hydraulic pressure required to move the dead weight [4].

The no-load tests were carried out with different driving frequencies and thicknesses of reed valve (0.05mm, 0.08mm, and 0.15mm). In these cases, the output piston was allowed to move freely and provide a maximum obtainable velocity

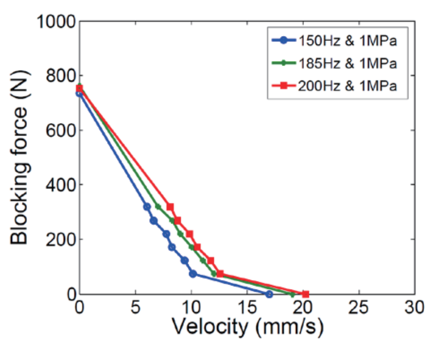

Fig. 11. Force-velocity diagram at 1MPa bias pressure and 0.05mm thickness of reed valve

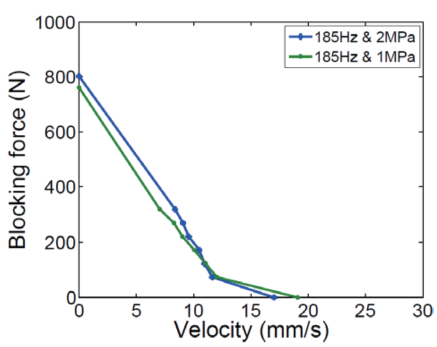

Fig. 12. Force-velocity diagram at 185Hz driving frequency and 0.05mm thickness of reed valve

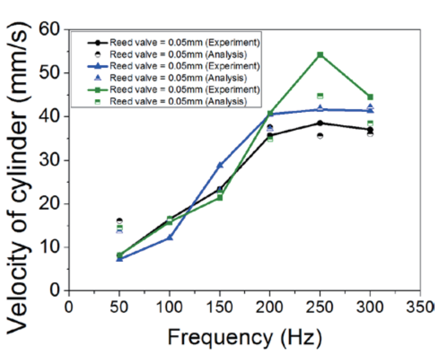

Fig. 13. Cylinder no-load velocity comparison of experiment and the simulation at 1MPa bias pressure

and flow rate from the hydraulic pump. The only opposing force was from friction between the output shaft and the inside wall of the hydraulic cylinder. Figure 13 shows that the maximum velocity was around 54.3mm/s when a 0.15mm reed valve was used at 200Hz and 1MPa bias pressure. The analysis results from ANSYS CFX13.0 software were also compared with the experiment result. The results of the analysis correlated well with the experimental results when 0.05mm and 0.08mm thickness of reed valve were used. However, when 0.15mm thickness of reed valve was used at 250Hz, the experiment result showed considerably higher values than when calculated numerically.

3.2 Test with Pst 1000/25/80 piezo-stack

Besides the PI P-025.40P piezo-stack, the Pst 1000/25/80 piezo-stack was also used to test the performance of the actuator. Figure 14 shows the maximum blocking force of the two kinds of piezo-stacks. In these measurements, the 0.05mm reed valve for measuring the maximum blocking force was selected. These results indicate that the system was very stable and the maximum blocking force was measured as 970.2N when the frequency was 185Hz. The power amplifier was automatically turned off when the frequency was higher than 250Hz because of its circuit protection inside.

Loading tests were also carried out under load to investigate the performance of the Pst 1000/25/80 piezo-stack. The experimental setup was the same as the performance testing of the P-025.40P piezo-stack. Figure 15 shows the force-velocity diagram of the two kinds of piezo-stacks when working with a 185Hz driving frequency, a 2MPa bias pressure, and a 0.05mm thickness of reed valve. For the Pst 1000/25/80 piezo-stack, the force was also inversely proportional to the velocity, and the curve had two folds, in which the bifurcation point was 7.5kg. This curve also went through the maximum force that was measured by the load cell.

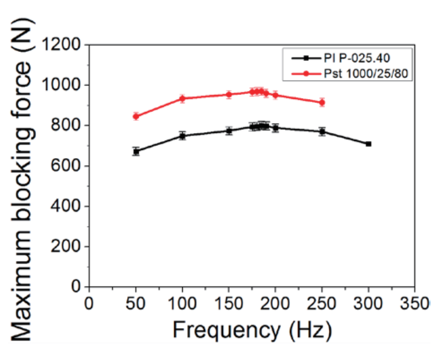

Fig. 14. Maximum blocking force of the two kinds of piezo-stacks at 2MPa bias pressure and 0.05mm thickness of reed valve

DOI: http://dx.doi.org/10.5139/IJASS.2015.16.4.520

The no-load test of the Pst 1000/25/80 piezo-stack was carried out with different driving frequencies, 0.15mm thickness of reed valve, and 1MPa bias pressure. Figure 16 shows the maximum velocity around 47.5mm/s when the working frequency was 250Hz.

Table 2 shows the comparison of the results before and after the improvement of the two piezo-stacks, P-025.40P and Pst 1000/25/80. After changing the design of the cylinder, the maximum no-load velocity was almost the same, but the maximum blocking force increased (5.6 times higher in the case of the P-025.40P piezo-stack). After changing the piezo-stack, the maximum no-load velocity decreased (12.5%), but the maximum blocking force increased (1.2 times higher). Therefore, decreasing the amount of air bubbles in the fluid was very important for the performance of the system, especially at the loading condition. The maximum blocking force was measured at 970.2N in this research when using the Pst 1000/25/80 piezo-stack and piezoelectric hydraulic actuator system (with new cylinder).

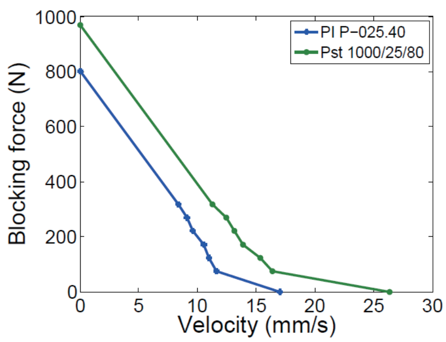

Fig. 15. Force-velocity diagram of the two kinds of piezo-stacks at 185Hz driving frequency, 2MPa bias pressure, and 0.05mm thickness of reed valve

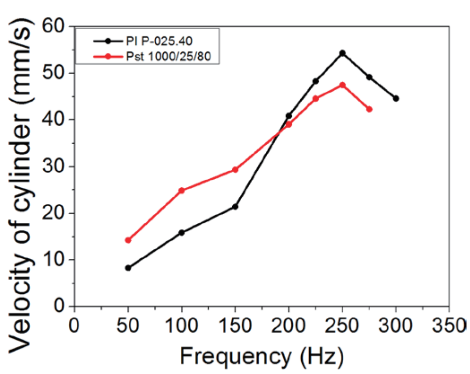

Fig. 16. No-load velocity comparison of the two kinds of piezo-stacks at 1MPa bias pressure and 0.05mm thickness of reed valve

Table 2. Comparison of the results before and after improvement

System performance	Preliminary result (P-025.40p)	Results after improvement (P-025.40p)	Results after improvement (Pst 1000/25/80)
Maximum velocity of output cylinder (mm/s)	50.9	54.3	47.5
Maximum blocking force of output cylinder (N)	142.5	801.3	970.2

4. Conclusion

In this research, a bidirectional piezoelectric hybrid actuator system was designed and manufactured. Two different types of piezo-stacks were used. The direction of the cylinder rod can be controlled using the LabVIEW program. In order to improve the performance of the system, the cylinder was enhanced and a load-cell measuring system was set up. The maximum velocity of the cylinder piston was measured to be 54.3mm/s when using a PI-025.40 piezo-stack, 0.15mm thickness of reed valve, and 1MPa bias pressure at a no-load condition. The numerical analysis result was also compared with the experiment result by using ANSYS CFX 13.0 software. The maximum blocking force was measured as 970.2N when using a Pst 1000/25/80 piezo-stack with 185Hz frequency, 0.05mm thickness of reed valve, and 2MPa bias pressure.

Acknowledgement

The authors would like to thank Prof. Norman M. Wereley, University of Maryland, United States, for his valuable comments and suggestions.

References

[1] Konishi, K., Yoshimura, T., Hashimoto, K., and Yamamoto, N., 1993, “Hydraulic Actuators Driven by

Piezoelectric Elements 1st Report, Trial Piezoelectric Pump and Its Maximum Power," Trans. Jpn. Soc. Mech. Eng., Ser. C, Vol. 59, No. 564, pp. 2477–2484.

[2] Sirohi, J., Cadou, C. and Chopra, I., "Investigation of the dynamic characteristics of a piezohydraulic actuator", *Journal of Intelligent Material Systems and Structures*, Vol. 16, No. 6, 2005, pp. 481-492.

[3] Ellison, J., *Investigation of active materials as driving elements in a hydraulic-hybrid actuator, Master Thesis*, University of Maryland, College Park, MD, USA, 2004.

[4] Chaudhuri, A., *Self-contained hybrid electro-hydraulic actuators using magnetostrictive and electrostrictive materials, PhD Thesis*, Department of Aerospace Engineering, University of Maryland, College Park, MD, 2008.

[5] Mauck, L. D. and Lynch, C. S., "Piezoelectric hydraulic pump development", *Journal of Intelligent Material Systems and Structures*, 2000, pp. 758-764.

[6] John, S., Chaudhuri, A. and Wereley, N.M., "Investigation of the dynamic characteristics of a piezohydraulic actuator", *Journal of Intelligent Material Systems and Structures*, Vol. 132, No. 2, 2010, pp. 021006-17.

[7] Xuan, Z. F., Jin, T. L., Ha, N. S., Goo, N. S., Kim, T. H., Bae, B. W., Ko, H. S. and Yoon, K. W., "Performance of piezo-stacks for a piezoelectric hybrid actuator by experiments", *Journal of Intelligent Material Systems and Structures*, Vol. 21, No, 18, 2014, pp. 2212-2220.

[8] PI 2013 Ceramic Fundamentals of piezoelectric actuators.

[9] Tan, H., Hurst, W. and Leo, D., "Performance modeling of a piezohydraulic actuation system with active valves", *Smart materials and structures*, Vol. 14, No. 1, 2005, pp. 91-110.

[10] Pham, M. and Goo, N. S., "Development of a Peristaltic Micropump with Lightweight Piezo-Composite Actuator Membrane Valves", *International Journal of Aeronautical and Space Sicences*, Vol.12, No. 1, 2011, pp. 69-77

[11] Chaudhuri, A., Yoo, J. H. and Wereley, N. M., "Development of a hybrid magnetostrictive Hydraulic actuator", Smart Materials and Structures 18: 085019, 2009.

[12] William, E. H., *Piezohydraulic actuator design and modeling using a lumped-parameter approach, Master Thesis*, Diss. Virginia Polytechnic Institute and State University, 2002.

[13] Sirohi, J. and Chopra, I., "Design and development of a high pumping frequency piezoelectric-hydraulic hybrid actuator", *Journal of Intelligent Material Systems and Structures*, Vol. 14, No. 3, 2003, pp. 135-147.

[14] Kim, K., Shin, S., Lee, J., Yee, K. and Oh, S. "Toward a More Complete Analysis for Fluid-Structure Interaction in Helicopters", *International Journal of Aeronautical and Space Sicences*, Vol. 7, No. 2,2006, pp. 110-146.

[15] Kim, J. H., Lee, J. W., Park, S. H., Byun, D., Byun, Y. H. and Lee, C. "FSI (Fluid-Structure Interaction) Analysis for Harmonious Operation of High-Speed Printing Machine", *International Journal of Aeronautical and Space Sicences*, Vol. 9, No. 1, 2008, pp. 137-146.

[16] Cho, J. H., Goo, N. S., Xuan, Z. F., Yoon, K. W. and Ko, H. S., "Study on flow distribution inside integrated hybrid actuator", *Journal of Mechanical Science and Technology*, Vol. 28, No. 9, 2014, pp. 3583-3588.

[17] Blevins, R. D., "Formulas for Natural Frequency and Mode Shape", *Journal of Applied Mechanics*, Vol. 47, Issue 2, 1980, pp. 461.

[18] Herdic, S. L., *Development of piezo-hydraulic actuation systems technology for use on a helicopter tailing edge flap, Master Thesis*, Georgia Institute of Technology, Atlanta, GA, 2005.